Pressure Loading on Curved Leading Edge Wings in Supersonic Flow

Milton E. Vaughn Jr.*
U.S. Army Missile Command, Huntsville, Alabama
and
John E. Burkhalter†
Auburn University, Auburn, Alabama

An approximate method is developed which extends pressure distribution theories for wings of constant sweep to wings with curvilinear leading edges. Two cases are considered. In the first case of a predominantly subsonic leading edge, an analogy is made to a wing in conical flow. In the second case of a supersonic/subsonic leading edge, physical reasoning is used to approximate the flow regions on the wing with line-source solutions. An application is made to a wing of ogee planform, and comparisons with experimental data prove very favorable.

Nomenclature

c	= local chord
(c_1,s_1)	= point where Mach cone intersects wing leading edge
(c_2,s_2)	= point where leading edge sweep angle is tangent to Mach cone
ΔC_p	= pressure loading coefficient, $C_{p_L} - C_{p_U}$
$E(k)$	= complete elliptic integral of the second kind
I	= line source strength
m	= wing sweep parameter, $\beta/\tan\Lambda$
U	= freestream velocity
u,w	= nondimensional perturbation velocity components
x,y,z	= Cartesian coordinates, positive downstream, to the right of the flight direction, and upward, respectively
x',y',z'	= coordinates in $M_\infty = \sqrt{2}$ domain
α	= angle of attack
β	= Mach flow parameter, $\sqrt{M_\infty^2 - 1}$
Λ	= leading edge sweep angle
ξ,η	= nondimensional wing coordinates
ξ',η',ζ'	= variables along the x',y',z' axes

Subscripts

c	= conical wing used in subsonic wing analogy
o	= ogee wing planform
s	= sonic wing used in supersonic pressure analysis
I	= inboard part of wing between root chord and (c_1,s_1)
O	= outboard part of wing between (c_1,s_1) and (c_2,s_2)
T	= tip region of wing outboard of (c_2,s_2)
LE	= leading edge of wing
TE	= trailing edge of wing
L	= lower surface of wing
U	= upper surface of wing

Received Nov. 17, 1985; revision received Feb. 2, 1986.

*Aerospace Engineer. Member AIAA.
†Associate Professor, Aerospace Engineering Department. Member AIAA.

Introduction

WINGS with complex planforms or curved leading edges have certain aerodynamic characteristics which offer specific advantages over wings of constant leading and trailing edge sweep angles. It has been observed, for example, that at subsonic speeds, both ogee wing planforms and double-delta planforms exhibit a stable vortex phenomenon on the wing which reduces the aircraft landing speed.[1-3] It has also been observed that at supersonic speeds a wing with a curvilinear complex leading edge achieves a significant level of leading edge thrust which is not attainable by a wing of constant sweep.[4,5] The resulting reduction in required engine thrust and the consequent fuel savings are very desirable characteristics, particularly at cruise speeds. Although a double-delta leading edge may achieve some increase in performance over the straight configuration, the discontinuity in sweep produces a Mach cone which tends to decrease the lift over the wing while increasing the drag. A wing with a smoothly contoured leading edge avoids these pitfalls by virtue of the continuity of the sweep angle. The potential economic advantages of this configuration are obvious, particularly for the supersonic flight regime.

Since the required aerodynamic characteristics may be obtained by integrating the pressure loading on the wing, most of the modeling effort can be focused on the pressure distribution, which may be obtained from the velocity potential. Generally, most methods assume small perturbations and moderate supersonic Mach numbers so that linearized aerodynamics are assumed in solving for the velocity potential.

One of the first successful pressure modeling techniques was a general analytical approach developed in 1950 by Evvard.[6] Applicable to arbitrary planforms, the solution technique extends Puckett's method of modeling a nonlifting wing with point sources[7] to account for the upwash effects of subsonic leading and trailing edges at angle of attack. For a thin, flat wing Evvard found the upwash field between the subsonic leading edge and the foremost Mach line to be equivalent to the effects of that part of the wing producing the upwash field. This equivalence reduces the solution for the velocity potential to the integration of the source distribution over a series of parallelograms on the wing surface. While Evvard's theory has been successfully applied to obtain closed-form solutions for the velocity potential of planforms with straight leading edges,[8,9] no closed-form solutions have been derived for planforms of variable sweep, possibly owing to the difficulty in obtaining analytical solutions to the integral for the velocity potential.

A less general analytical approach was taken by Cohen and Friedman[10] in their development of closed-form solutions for the pressure loading on double-delta planforms. Their technique models the highly swept inboard portion of the wing with conical flow theory while the outboard portion is modeled by superimposing a mathematical solution which cancels the upwash due to the conical flow theory. This approach works well, except near the juncture of the two wing panels. As one approaches the juncture, the superimposed solution approaches $-\infty$ at a faster rate than the conical flow theory approaches ∞, thereby causing the pressure solution to be invalid.

As analytical methods have generally proved to be difficult to use, more easily applicable numerical techniques have been developed to analyze complex planforms. One successful numerical approach is Chin's method,[11] which extends Etkin's numerical integration technique for the velocity potential[12,13] to wings with curvilinear leading edges.

Etkin's approach is based on Evvard's theory but is restricted to wings with straight leading edges. Each leading edge of the wing must be either completely subsonic or completely supersonic; however, one leading edge may be subsonic while the other one is supersonic, as in the case of the yawed wing. By restricting the integration to the two parallelograms immediately upstream of the point in question, Etkin greatly simplified the integration for the velocity potential. He further simplified the procedure by using a computation grid formed of a uniform network of small parallelograms in which he assumed the wing flow properties to be constant. It is this simplified numerical integration technique that Chin extended to wings with curved leading edges.

By using an inverse function of the equation of the leading edge, Chin was able to determine the dimensions of the parallelograms upstream of the point in question, thus extending Etkin's technique to wings with curvilinear planforms. He then applied Ward's modification of Evvard's early work[14] and observed that the velocity potential for a wing with a partially subsonic and partially supersonic leading edge was equal to the potential for a completely subsonic leading edge plus the potential for a completely supersonic leading edge. Hence, Chin was able to extend Etkin's numerical integration technique to wings having each leading edge, both subsonic and supersonic. Chin's method has been applied to a wing of ogee planform with very reasonable results.[15]

A different numerical method which utilizes supersonic vortex lattice theory was developed in 1974 by Carlson and Miller.[16] Applicable to arbitrary planforms, this integration technique employed a rectilinear computational grid system of wing elements and used numerical weighting factors to permit better definition of the wing planform in the grid system. Carlson and Miller assumed the wing element properties to be constant and allowed the integration to proceed over the entire wing surface contained within the forecone; however, the method produced severe oscillations in the pressure coefficient at given spanwise stations so that it was necessary to manipulate the data with a smoothing technique. Originally, Carlson and Miller used a nine-point smoothing function which required four grid elements aft of the wing trailing edge. Later, however, an aft-element sensing technique was employed which required only one additional grid element. Comparisons made with linearized theory have proved to be favorable.

Finally, one additional technique, employed by Burkhalter,[17,18] utilized a combination of the basic Evvard theory[6,8,9] and a doublet paneling approach (similar to the vortex lattice method of Carlson and Miller) to model the off-design or nonplanar aspects of thin finite wings. Although not applied to curved wings per se, the method is applicable to both subsonic and supersonic leading edges and does not exhibit the numerical oscillations observed in other techniques. Comparison of the method with missile wind tunnel data has proved very favorable.

Although numerical approaches are useful design tools, it is economically advantageous and nearly as accurate to use approximate analytical solutions for at least the preliminary design phase of an aircraft or missile. Such a preliminary design tool is used in the method of Cohen and Friedman for double-delta wings, and in the method of Burkhalter for nonplanar configurations, but no such approach is available for a wing with a curved leading edge. It is the intent of the present work to develop an analytical design tool for a wing with a curved leading edge.

Basicially there are two cases to be considered: One is when the wing is completely contained in the Mach cone emanating from the wing apex, and the other is when the wing leading edge is intersected by the Mach cone. Using simplifying engineering approximations, conical flow theory[20] and Jones' line-source method[22] (both originally derived for wings with straight leading edges) can be extended to a thin, flat, lifting supersonic wing with curved leading edges and supersonic trailing edges. In the first case of a wing completely contained in the apex Mach cone, i.e., a subsonic leading edge, an analogy is made to a wing in a conical flow. For the second case of a partially subsonic and partially supersonic leading edge, physical reasoning is used to approximate the flow regions on the wing with line-source solutions. The analysis is developed for an ogee planform, and small perturbations are assumed.

Theory

For the two cases previously introduced, the theory is developed for the wing alone. The effects of the body of the wing can be taken into account using lift ratios or by other methods (see, e.g., Ref. 19). Moderate supersonic Mach numbers and small perturbations are assumed so that potential flow techniques may be utilized in the analysis.

Case I: Wing Contained in Mach Cone

A typical wing with a straight leading edge contained within the Mach cone is shown as the solid wing in Fig. 1. The leading edges are subsonic because the velocity component normal to each leading edge has a Mach number less than unity. The wing is formed by the sweep of a ray emanating from the vertex of the Mach cone, and the flow properties are constant along any given ray within the Mach cone (the conical condition), including those rays along the body.[20] Such a wing is said to be a conical body because it satisfies the conical condition.[20,21] From conical flow theory,[21] which is commonly used to determine the pressure loading on such a wing, the pressure difference at a point (x,y) on the wing is given by

$$\Delta C_p = 4\alpha / [E(k)(\tan \Lambda)\sqrt{1-t^2}] \tag{1}$$

where

$$t = (y \tan \Lambda)/x \tag{2}$$

and $E(k)$ is the elliptic integral of the second kind, with

$$k = \sqrt{1-(\beta^2/\tan^2 \Lambda)} \tag{3}$$

and the origin of the reference axes lies on the apex of the wing. Equation (1) accounts for all possible influences on the point, including those of the opposite semiwing. If it is now assumed that the leading edges are curved and subsonic, as shown by the dashed line in Fig. 1, then the flow properties change across the leading edge and conical flow theory is no longer applicable. However, an analogy can be made between the variable swept wing and some "equivalent" conical wing. It is observed that at any given spanwise station, there is basically little qualitative difference between a conical wing and a "subsonic" curved wing. Both wings have stagnation points at the leading edge, and both have supersonic trailing edges which sustain a pressure loading. Moving downstream along the chords of both wings, the areas of integration include increasingly larger portions of the subsonic leading edges so that one might expect the pressure curves to be similar in shape. More specificially, since the conical wing exhibits a subsonic type of pressure curve, one would anticipate the curved wing also to have a subsonic type of pressure curve.

The closest quantitative analogy to a given wing with curvilinear leading edges is probably a conical wing that completely circumscribes the curved wing, as shown in Fig. 1. The only deviations from the curvilinear planform, then, are the straight leading edges of the conical wing. By assuming that the nondimensional chordwise pressure distribution is approximately the same for both wings at a given spanwise location, conical flow theory may be extended to the curved planform. The extension of conical flow theory is achieved by application of the nondimensional chordwise variable ξ_0 to the chord of the encompassing conical wing. The pressure loading at any point (x,y) on the curved wing would then be given by

$$\Delta C_p = 4\alpha / [E(k)(\tan \Lambda_c)\sqrt{1-t^2}] \tag{4}$$

where

$$t = (y \tan \Lambda_c)/x_c \tag{5}$$

$$x_c = x_{\mathrm{LE}_c} + \xi_0 c_c \tag{6}$$

and

$$k = \sqrt{1-(\beta/\tan \Lambda_c)^2} \tag{7}$$

As a clarifying example, consider the wings shown in Fig. 2. The conical wing in Fig. 2b was obtained by circumscribing the curvilinear planform shown in Fig. 2a. It is assumed that the nondimensional pressure curves for both wings at $\eta = 0.50$ (shown in Fig. 2) are approximately the same so that the unknown pressure difference at $\xi_0 = 0.25$, for example, is the same as the known pressure value at $\xi_c = 0.25$. To determine the pressure loading at point A on the curved wing, then, one would first use Eq. (6) to determine the location of $\xi_0 = A$ as it occurs on the analogical conical wing, as shown by point A_c. Since the pressure at $\xi_0 = A$ is assumed to be the same as that at $\xi_c = A_c$, the pressure loading at point A is determined by predicting the loading at point A_c with conical flow theory, Eqs. (4)-(6).

If the analogical conical wing has a nonzero tip chord, it is assumed that no significant tip effect occurs on the curved wing, i.e., the pressure difference is not reduced by the effects of the underside of the wing. As shown schematically in Fig. 3, the curved tip provides a mechanism for the vortex flow to initiate gradually along the leading edge rather than abruptly, as for the streamwise tip. This mechanism provides for a vortex-induced reattachment of the flow and prevents separation.

It is recognized that all continuously curved wings contained within the Mach cone will not have subsonic leading edges all along the span. It is assumed, however, that if supersonic leading edges exist for a particular planform shape, these regions will lie along the outboard portion of the wing. In this case, it is presumed that upstream subsonic influences (such as the effect of the underside of the wing at the inboard portion of the wing) tend to modify the pressure

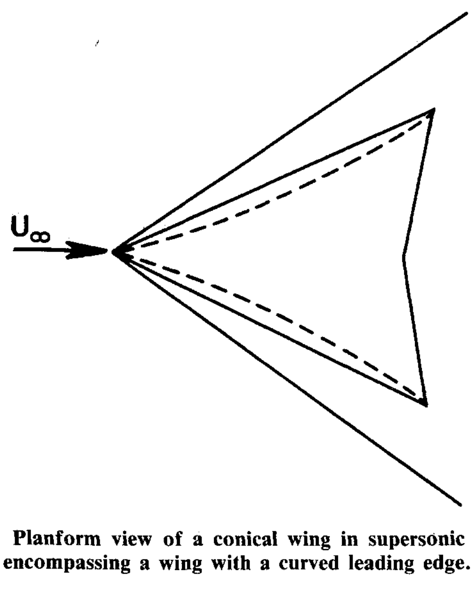

Fig. 1 Planform view of a conical wing in supersonic flow completely encompassing a wing with a curved leading edge.

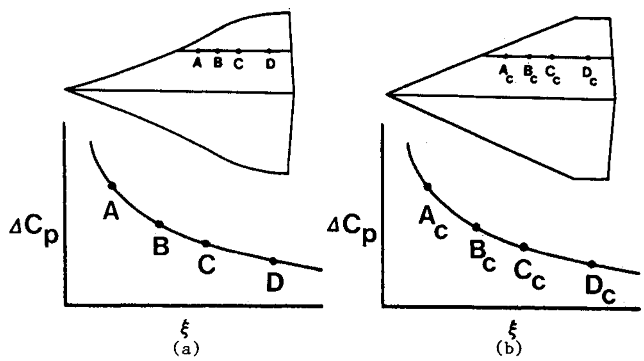

Fig. 2 Pressure curves for the conical wing analogy example.

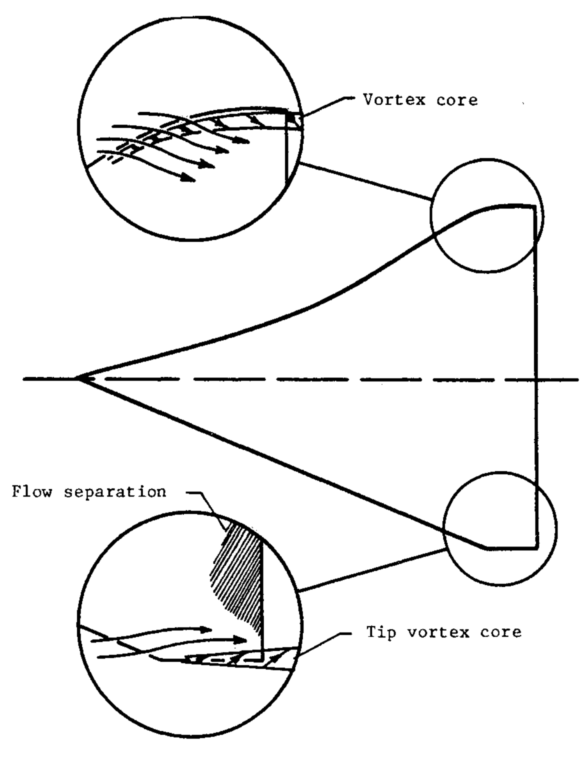

Fig. 3 Schematic comparison of a curved-tip vortex with a streamwise-tip vortex.

distribution along the chord such that it more nearly resembles a subsonic distribution.

Case II: Wing Intersected by Mach Cone

In off-design conditions when the Mach cone intersects the leading edge of the wing, another Mach cone is formed at the point of intersection. This new Mach cone divides the planform into regions of flow, as shown in Fig. 4 for an ogee planform. Similar regions of flow would occur for any wing with a sweptback, continuously curved leading edge and a highly swept inboard section. In analyzing the resultant flowfield, one must deal with mixed types of flows, because the leading edge is both subsonic and supersonic to significant degrees. Whereas region 1, the outboard leading edge ahead of the Mach cone, is supersonic, region 2, the inboard leading edge within the Mach cone, is both partially subsonic and partially supersonic. Region 3 is influenced by the opposite semiwing and by both regions 1 and 2. Region 4 is also influenced by the opposite semiwing, as well as by regions 1, 2, and 3. The dashed lines tangent to the Mach cone of the wing apex indicate the region of the tip effect. Although analyzing these interacting mixed flows presents quite a problem, a few logical assumptions produce a relatively simple solution technique for the wing alone.

In region 1, the varying sweep of the leading edge would cause an infinitesimally thin wing to have various degrees of pressure loading at the leading edge. In particular, the pressure loading would increase with increasing sweep, as evidenced by Puckett's formula for supersonic leading edges[7]:

$$\Delta C_p = 4\alpha / [U_\infty \sqrt{\beta^2 - \tan^2 \Lambda}] \tag{8}$$

However, it must be noted that one is dealing with a real wing having a certain thickness. At or very near the leading edge, one is likely to observe pressures slightly higher than predicted owing to the thickness of the wing and the shape of the airfoil cross section. Also notice that as one moves in the chordwise direction (Fig. 5a) the points in question are increasingly influenced by the more highly swept inboard part of the supersonic leading edge. The higher pressure loadings of these inboard influences should tend to increase the loading at the point in question. All things considered, then, it does not seem unreasonable to approximate the supersonic leading edge ahead of the Mach line by an appropriate straight leading edge. The approximating straight leading edge would extend from the intersection of the wing with the Mach cone to the point of tangency with the Mach cone at the tip, as shown in Fig. 5b.

In region 2, it may be observed that while the leading edge is both subsonic and supersonic, the supersonic portion will be influenced by the upstream subsonic part of the wing. As previously explained, this influence should cause the flow to behave somewhat subsonically. With the reasoning of the previous section, the pressure distribution of region 2 should be approximately modeled by analogy to a wing with a sonic leading edge at its inboard portion which will encompass the inboard section of the curved wing (see Fig. 5c). Conical flow theory is not necessary, but if another technique is used, it must take into account the opposite semiwing.

Consider now the flow regions on the rest of the wing. With the previous approximations the flow in region 3 may be considered as the flow aft of a Mach line on a wing with a straight supersonic leading edge as affected by the upstream influence of a sonic leading edge. The total pressure loading in region 3 can therefore be determined by superimposing the contributions from regions 1 and 2 and from the opposite semiwing. The same approach can be applied to region 4, with the additional contribution of region 3 to be considered. The region of tip effect will be discussed later.

The basic solution scheme has been discussed, but the question remains as to how to model the flow in the various

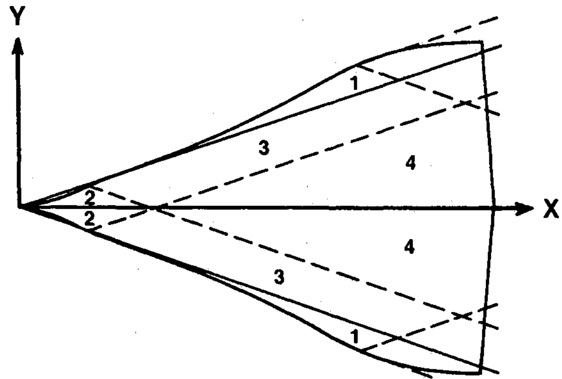

Fig. 4 Ogee wing intersected by a Mach cone.

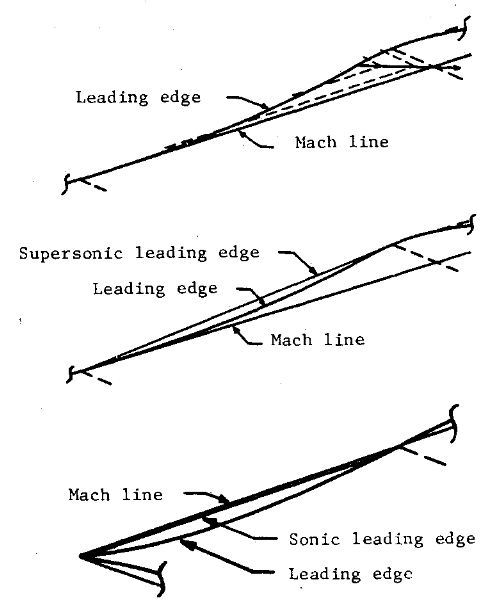

Fig. 5 Details of curved leading edge/Mach line considerations.

regions on the wing mathematically. The flow in region 1 could be modeled by Harmon-Jeffreys' theory,[8] but the derivation includes the effect of an opposite supersonic semiwing. The opposite semiwing is subsonic with respect to region 3, so the solution is inapplicable there. The conical flow technique used in the previous section could model the flow in region 2, but conical flow assumes the entire wing to have a subsonic leading edge so region 3 would again be improperly modeled. A modeling technique that is compatible with the simplifying assumptions, as well as the physical character of the planform, is the line-source theory of Jones,[22] which is discussed below.

Region 1

By transforming the small perturbation equation to the $M_\infty = \sqrt{2}$ domain, Jones derived the longitudinal velocity component of an oblique line source lying along a supersonic leading edge as

$$u = I\cos^{-1}(x' / \sqrt{y'^2 + z'^2}) \tag{9}$$

where

$$x' = x - m\beta y$$

$$y' = \beta y - mx$$

$$z' = \beta z - mx \tag{10}$$

$$m = \beta / \tan \Lambda \tag{11}$$

determine the location of the point (x,y) on the transformed wing, and I is the strength of the line source. (See Fig. 4 for the orientation of the coordinate system.) Jones also derived the boundary condition equation by which the source strength may be determined. This boundary condition equation is given as

$$w = -\pi I\sqrt{m^2-1/m} \tag{12}$$

where w is the induced wing downwash. For a thin planar wing, the boundary condition of no flow through the wing can be approximated by

$$w+\alpha \doteq 0 \tag{13}$$

so the source strength is found to be

$$I = m\alpha/(\pi\sqrt{m^2-1}) \tag{14}$$

Now the small perturbation pressure coefficient is given by

$$C_p = 2u/U_\infty \tag{15}$$

so that for a planar wing the pressure difference is given by

$$\Delta C_p = 2C_{p_L} = 4(u/U_\infty) \tag{16}$$

Using the supersonic similarity rule[23] given by

$$C_p = (1/\beta)C_p\,|_M = \sqrt{2} \tag{17}$$

one may utilize Eqs. (10), (15), and (17) to obtain

$$\Delta C_p = 4\alpha m/(U_\infty \pi\beta\sqrt{m^2-1})\cos^{-1}\left(\frac{x'}{|y'|}\right) \tag{18}$$

for an oblique line source lying along a supersonic leading edge. Equation (18) holds only for points aft of the Mach line. In crossing ahead of the Mach line, Jones found that

$$u = I\pi \tag{19}$$

so that

$$\Delta C_p = 4\alpha m/(U_\infty \beta\sqrt{m^2-1}) \tag{20}$$

for points ahead of the Mach line. Although Jones' line-source theory was derived for nonlifting wings, the independence of the flowfield on the upper and lower surfaces of the wing permits the use of the theory for lifting wings.

Region 2

Jones also derived the longitudinal velocity component for an oblique line source lying along a subsonic leading edge to be

$$u = I\cosh^{-1}(x'/\sqrt{y'^2+z'^2}) \tag{21}$$

with the boundary condition equation given by

$$w = -\pi(I/m)\sqrt{1-m^2} \tag{22}$$

If the x coordinate used in Eq. (10) is given by

$$x = x_{\mathrm{LE}_s} + \xi_0 c_s \tag{23}$$

the previously mentioned analogy is made to a wing with a sonic leading edge, which should provide for a better representation of the subsonic character of the flow. Using the previous reasoning, one finds that

$$\Delta C_p = 4\alpha m/(U_\infty \pi\beta\sqrt{1-m^2})\cosh^{-1}\left(\frac{x'}{|y'|}\right) \tag{24}$$

for an oblique line source lying along a subsonic leading edge. The value of m in Eq. (24) is restricted by

$$m<1 \tag{25}$$

which is equivalent to saying that the Mach line lies slightly upstream of the wing leading edge.

The line-source solution of Eq. (24) accounts only for the effects of the right semispan on point (x,y). Consequently, one must properly take into account the effect of the left semiwing. For a symmetric planform, using a mirror image of point (x,y)—i.e., $(x,-y)$—in Eq. (24) determines the pressure effect of the opposite semiwing. For a nonsymmetric planform, another technique must be employed. Regardless, superposition of the effect of the opposite semiwing onto the solution of Eq. (24) at (x,y) will predict the total pressure loading at point (x,y).

Since line-source theory was originally developed for wings of zero lift, the flow interaction between the upper and lower surfaces of subsonic wings was not taken into account; however, the assumption of a sonic leading edge for the analogical wing rules out any such interaction, and Jones' line-source theory therefore becomes applicable.

Region 3

While Eqs. (20) and (24) respectively determine the pressure loading in regions 1 and 2, linear superposition of solutions must be used in region 3. By calculating the effect of a sonic line source from the wing apex to the limit of the forecone of integration and then subtracting the effect of a sonic line source from point (c_1,s_1) to the same limit of the forecone (see Fig. 6), one may approximate the effect of the sonic inboard part of the wing on point (x,y). Then, using Eq. (18) to determine the contribution of the supersonic leading edge, one may superimpose the pressure effects on point (x,y). Mathematically, this may be represented as

$$\Delta C_p = \frac{4\alpha}{U_\infty \pi\beta}\left\{(m_I/\sqrt{1-m_I^2})\left[\cosh^{-1}\left(\frac{x'}{|y'|}\right) - \cosh^{-1}\left(\frac{x'-\xi'}{|y'|}\right)\right] + (m_O/\sqrt{m_O^2-1})\cos^{-1}\left(\frac{x'}{|y'|}\right)\right\} \tag{26}$$

where

$$m_I = \beta/\tan\Lambda_I \tag{27}$$

$$m_O = \beta/\tan\Lambda_O \tag{28}$$

and

$$\xi' = c_1 - m_I\beta s_1 \tag{29}$$

with (c_1,s_1) locating the point where the Mach cone intersects the leading edge of the wing. As with region 2, the line-source solution of Eq. (26) accounts for only the influence of

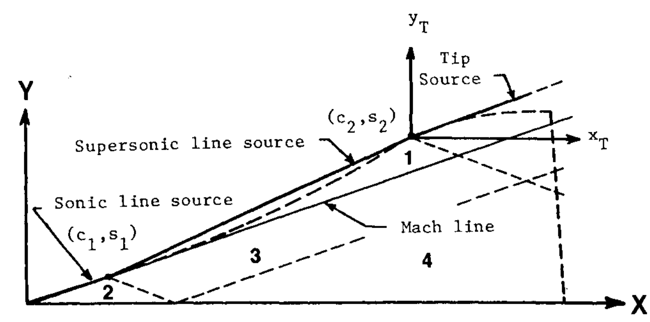

Fig. 6 Line-source model for the right semispan of an ogee wing.

the right semispan on the point in question. Therefore, for a symmetric planform, the total pressure loading at point (x,y) is obtained by superposition of the solution of Eq. (26) at $(x-y)$.

Region 4

The solution technique for points in region 4 is exactly the same as for points in region 3 of the wing. The only difference is that while only the opposite sonic line-source solution affects points in region 3, both the sonic and supersonic line-source solutions of the opposite semiwing affect points in region 4.

Region of Tip Effect

Assuming for the moment that the Mach cone intersects the wing at only one point (c_1,s_1), one would expect to have a pressure drop where the leading edge sweep angle becomes greater than β near the tip; however, as mentioned in the analysis of case I, the curvature of the tip is such that vortex flow is initiated along the leading edge, which provides for a vortex-induced reattachment of the flow and prevents separation. Consequently, one would not find a pressure drop near the tip but, rather, a subsonic type of behavior.

One might attempt to approximate the subsonic behavior with a localized conical flow solution superimposed on the other supersonic and sonic influences; however, a conical flow solution would inherently assume that the inboard Mach line originating at the tip constitutes the leading edge of a conical airfoil, which is not the case.

In the interest of approximately modeling the flow, then, another sonic line source is placed at the point of tangency with the Mach line (c_2,s_2). Using the procedure developed for region 2, the pressure loading is determined and then additional upstream influences are superimposed. The basic pressure function for the tip region is

$$\Delta C_p = (4\alpha m_T)/(U_\infty \pi\beta\sqrt{1-m_T^2})\cosh^{-1}(x'_T/|y'_T|) \tag{30}$$

where

$$x'_T = x - c_2 - m_T\beta(y-s_2)$$

$$y'_T = \beta(y-s_2) - m_T(x-c_2) \tag{31}$$

and, as with region 2,

$$m_T < 1 \tag{32}$$

The resulting wing model is shown in Fig. 6. For points outboard of $\eta = s_2$, a better pressure modeling may be obtained by using the wing analogy of case I such that the x coordinate in Eq. (31) would be given by Eq. (23) as

$$x = x_{\mathrm{LE}_s} + \xi_0 c_s \tag{33}$$

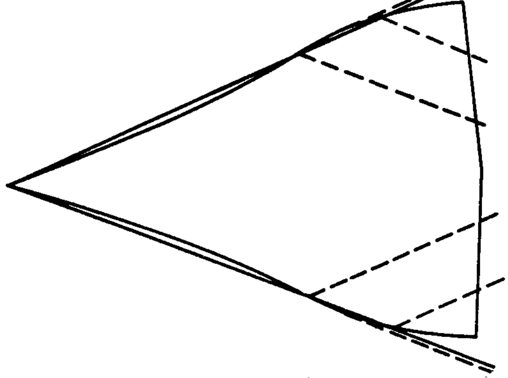

Fig. 7 Leading edge intersected by a Mach cone at two points.

All x'-y' coordinates are referenced to point (c_2,s_2) in the tip analysis.

In the case where the Mach line intersects the wing twice, as shown in Fig. 7, the flow-preserving vector phenomena should occur again. It is approximated that the Mach line will exert a minimal effect on the subsonic character of the vortex phenomena such that one would use the foregoing tip analysis to approximate the loading at the tip.

Results

Comparison of theory with available experimental pressure data[24] for a flat ogee wing (Fig. 8) are shown in Figs. 9-11. As previously stated, the body effects are taken into account through the use of lift ratios,[19] which have been shown to be

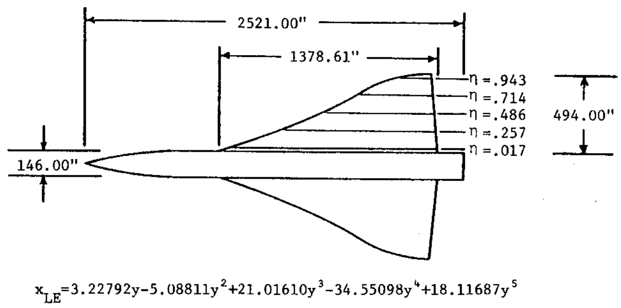

Fig. 8 Ogee wing-body configuration details.

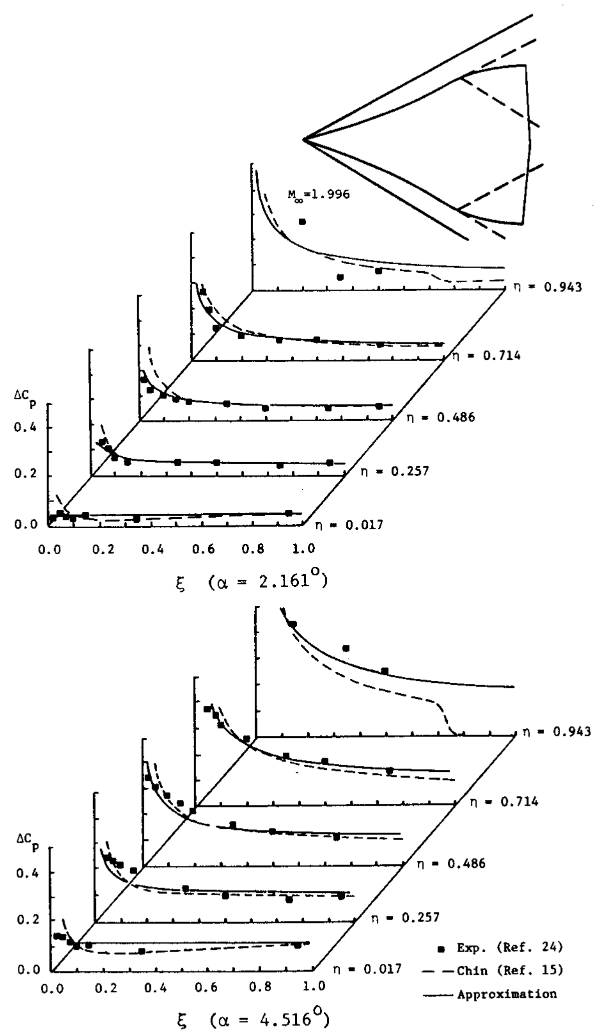

Fig. 9 Pressure loading on an ogee wing-body configuration with $M_\infty = 1.996$, $\alpha = 2.161$ deg, and $\alpha = 4.516$ deg.

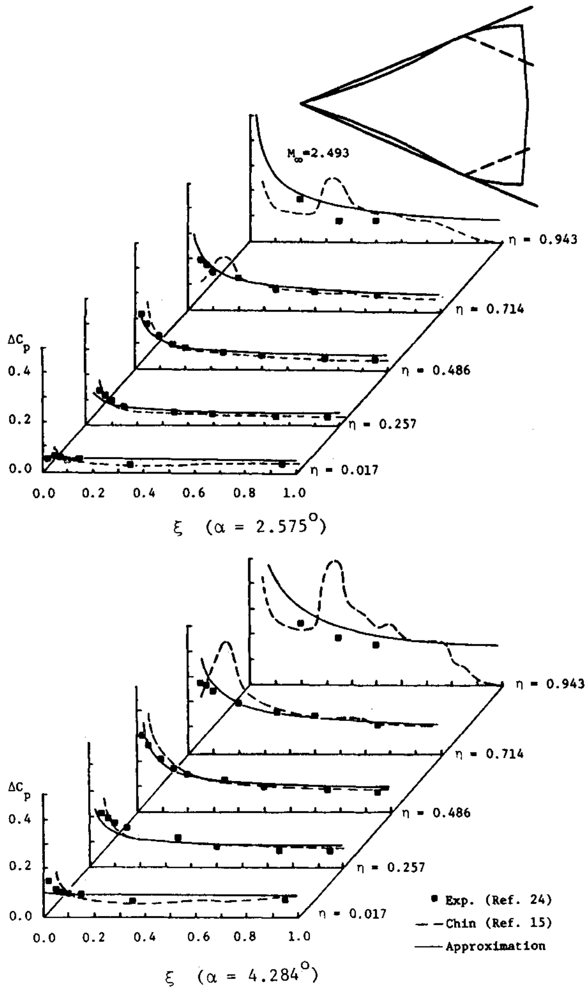

Fig. 10 Pressure loading on an ogee wing-body configuration with $M_\infty = 2.493$, $\alpha = 2.575$ deg, and $\alpha = 4.284$ deg.

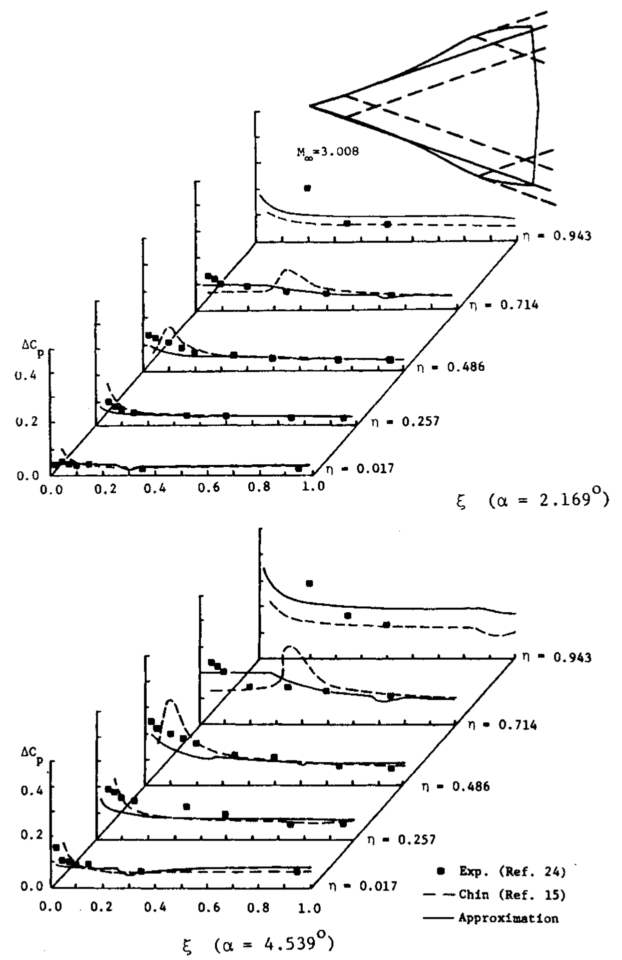

Fig. 11 Pressure loading on an ogee wing-body configuration with $M_\infty = 3.008$, $\alpha = 2.169$ deg, and $\alpha = 4.539$ deg.

valid for moderate supersonic Mach numbers. Comparison with Chin's method applied to the same wing is also shown. Although Crotsley's report,[15] from which Chin's data were taken, did not account for body effects in the pressure data, the body effects would simply increase the predicted pressure loadings. Additionally, the spanwise stations were measured from the wing-body centerline by Crotsley, whereas they were measured from the wing root in this report, resulting in the unusual values for the spanwise stations.

Results for case I conditions are presented in Figs. 9 and 10. It can be seen that the postulated "conical" behavior of the pressure curves is borne out quite well. The most significant deviations with experimental data occur at the tip. Even here, however, the agreement with the approximation is quite good at an angle of attack of about 4 deg. The unusual subsoniclike behavior at the tip seems to indicate the presence of the postulated vortex phenomenon which preserves the pressure, rather than a tip effect in which the pressure loading would be near zero.[9] The pressure drop at $M_\infty = 1.996$ and $\alpha = 2.161$ deg does not seem to be due to a Mach line originating near the tip, because the point is far aft of such an occurrence. The theory slightly underpredicts the data for $M_\infty = 1.996$ and $\alpha = 4.516$ deg at $\eta = 0.2571$ and $\eta = 0.4857$, but the approximation compares favorably with Chin's method.

The results for case II are shown in Fig. 11. The approximation compares favorably with the experimental data, although it does seem to underpredict the pressures at $\eta = 0.257$ and $\eta = 0.486$. The underprediction is probably a result of using a constant sweep angle from the point of intersection with the Mach line to the point of tangency with the Mach line. The increased sweep of the inboard sections of the wing would contribute to a pressure loading higher than predicted at these spanwise stations. There may also be some separation phenomena that cannot be taken into account by potential flow theories. In particular, note Chin's similar underprediction for $\alpha = 4.539$ deg at $\eta = 0.257$.

It was observed that as one moved further outboard, the chordwise points tended to lie closer and closer to the Mach line, which is itself coincident with the superimposed sonic sources. Numerical inaccuracies in the computer caused the sonic contribution to be overcalculated and it was observed that the overcalculation occurred when $x'/|y'|$ of the original sonic sources exceeded $x'/|y'|$ of the superimposed sonic source by a value of 0.00011. The sonic contribution should have decreased as one moved further outboard on the wing, but such a decrease did not occur immediately aft of the Mach line. Additionally, the sonic contribution should have been small immediately aft of the Mach line, but this was not the case. The overprediction did not occur when checks were made by other methods and the overprediction occurred only at one or two points just aft of the Mach line and past $\eta = 0.50$ on the wing. The expected behavior was exhibited at all other points on the wing, so the overprediction was deduced to be the result of numerical inaccuracies in the computer. To avoid this overcalculation, the difference in the $x'/|y'|$ parameters was artificially kept to a maximum of 0.00011. Prior to any corrections being made, it was observed that the difference in the $x'/|y'|$ parameters was less than 0.00011 all along the wing, except near the Mach line for $\eta = 0.7143$ and $\eta = 0.9429$.

The discrepancy at the leading edge for $\eta = 0.7143$ is probably due to leading edge thickness. The approximation agrees well with the experimental data for $\alpha = 2.169$ deg, so that the disagreement at $\alpha = 4.539$ deg seems to be due to some unusual pressure-reducing phenomenon occurring ahead of the Mach line, possibly some sort of sidewash phenomenon. The tip appears to have subsonic characteristics without significant pressure drop, thus confirming the pressure-preserving vortex phenomena. The behavior of the experimental data also indicates that the behavior is not sonic, so some refinement might be made of the theory at the tip for case II.

The various dips in the theoretical curves are due to pressure losses occurring at Mach lines, followed by gradual increases in pressure loading due to the contribution of the inboard sonic part of the wing model. The "bump" at $\eta = 0.4857$ and $\xi = 0.275$ is due to the rate at which the sonic and supersonic solutions sum together in the model. Again, notice the favorable comparisons of the approximation with Chin's method.

Conclusions

A successful analytical approximation has been developed which extends theories for wings of constant sweep to a wing of ogee planform. Very favorable comparison has been observed with both experimental data and Chin's numerical method. Agreement seems to be most favorable for wings completely contained within the Mach cone, which is the design condition for most supersonic cruise planforms. It must be noted, however, that the off-design conditions of the case II circumstances are reasonably well predicted by the approximation. Computing time is minimal, less than 5 s per run on an IBM 3033, and, since ΔC_p is obtained analytically, this method requires only one integration over the wing to obtain the total loading. Other techniques, as described in Refs. 11 and 16, however, may require additional integration passes, smoothing routines, and inversions of large matrices. The simplicity of this method (including run time and computer storage requirements) makes it easily adaptable to personal computers. It could easily be applied to other wings of curvilinear planform with highly swept inboard portions, thus providing the aerodynamicist with a reasonably accurate, quick, and inexpensive design tool. Extension of the method could be made to cambered wings, utilizing the method of Burkhalter, and to finite wing-body combinations to more accurately predict total configuration loads and moments.

Acknowledgments

This work was partially sponsored by the U.S. Army Missile Command, the Army Research Office under Contract DAAG29-78-G-0036, and by the Auburn University Engineering Experiment Station.

References

[1]Spence, A. and Smith, J. H. B., "Some Aspects of the Low-Speed and Supersonic Aerodynamics of Lifting Slender Wings," *Proceedings of the International Council of the Aeronautical Sciences,* Third Congress, Stockholm, 1962, pp. 553-568.

[2]Rolls, L. S., Koenig, D. G., and Drinkwater, F. J., III, "Flight Investigation of the Aerodynamic Properties of an Ogee Wing," NASA TN D-3071, Dec. 1965.

[3]Wentz, W. H., Jr., and McMahon, M. C., "An Experimental Investigation of the Flow Fields about Delta and Double-Delta Wings at Low Speeds," NASA CR 521, Aug. 1966.

[4]Robins, A. W., Carlson, H. W., and Mack, R. J., "Supersonic Wings with Significant Leading-Edge Thrust at Cruise," NASA TP 1632, April 1980.

[5]Robins, A. W., Lamb, M., and Miller, D. S., "Aerodynamic Characteristics at Mach Numbers of 1.5, 1.8, and 2.0 of a Blended Wing-Body Configuration With and Without Integral Canards," NASA TP 1427, May 1979.

[6]Evvard, J. C., "Use of Source Distributions for Evaluating Theoretical Aerodynamics of Thin Finite Wings at Supersonic Speeds," NACA Rept. 951, 1950.

[7]Puckett, A. E., "Supersonic Wave Drag of Thin Airfoils," *Journal of the Aeronautical Sciences,* Vol. 13, 1946, pp. 475-484.

[8]Harmon, S. M and Jeffreys, I., "Theoretical Lift and Damping in Roll of Thin Wings with Arbitrary Sweep and Taper at Supersonic Speeds—Supersonic Leading and Trailing Edges," NACA TN 2114, May 1950.

[9]Malvestuto, F. S., Jr., Margolis, K., and Ribner, H. S., "Theoretical Lift and Damping in Roll of Thin Sweptback Wings of Arbitrary Taper and Sweep at Supersonic Speeds—Subsonic Leading Edges and Supersonic Trailing Edges," NACA TN 1860, April 1949.

[10]Cohen, D. and Friedman, M. D., "Theoretical Investigation of the Supersonic Lift and Drag of Thin, Sweptback Wings with Increased Sweep Near the Root," NACA TN 2959, June 1953.

[11]Chin, C. L. D., "Extension of Evvard-Etkin Load Prediction Technique," North American Aviation, Inc., Los Angeles, CA, NA-63-931, Sept. 1963.

[12]Etkin, B. and Woodward, F. A., "Lifting Distribution on Supersonic Wings with Subsonic Leading Edges and Arbitrary Angle of Attack Distribution," *Journal of the Aeronautical Sciences,* Vol. 21, 1954, pp. 783-785.

[13]Etkin, B., "Lift Distribution on Warped Supersonic Wings," *Canadian Aeronautics and Space Journal,* April 1955, pp. 16-20.

[14]Ward, G. N., "Supersonic Flow Past Thin Wings, I. General Theory," *Quarterly Journal of Mathematics and Applied Mechanics,* Vol. 2, 1949, pp. 136-152.

[15]Crotsley, H. H., "An Analysis of Wing Tunnel Pressure Distributions and a Comparison of Experimental and Theoretical Methods for Two Ogee Wing-Body Configurations with and without Twist and Camber," North American Aviation, Inc., Los Angeles, CA, NA-63-1445, Dec. 1963.

[16]Carlson, H. W. and Miller, D. S., "Numerical Methods for the Design and Analysis of Wings at Supersonic Speeds," NASA TN D-7713, Dec. 1974.

[17]Burkhalter, J. E., "Load Distribution on Deformed Wings in Supersonic Flow," *Journal of Aircraft,* Vol. 19, Nov. 1982, pp. 921-927.

[18]Burkhalter, J. E., "Prediction of Missile Aerodynamic Coefficients," Final Report, U.S. Army Missile Command, Missile Intelligence Agency, Sept. 1985.

[19]Nielsen, J. N., Kaattari, G. E., and Anastasio, R. F., "A Method for Calculating the Lift and Center of Pressure of Wing-Body-Tail Combinations at Subsonic, Transonic, and Supersonic Speeds," NACA RM A53G08, Nov. 1953.

[20]Lagerstrom, P. W., "Linearized Supersonic Theory of Conical Wings," NACA TN 1685 (Corrected Copy), Jan. 1950.

[21]Stewart, H.J., "The Lift of a Delta Wing at Supersonic Speeds," *Quarterly of Applied Mathematics,* Vol. IV, Oct. 1946, pp. 246-254.

[22]Jones, R. T., "Thin Oblique Airfoils at Supersonic Speed," NACA Rept. 851, 1946.

[23]Ashley, H., and Landahl, M. T., *Aerodynamics of Wings and Bodies,* 1st ed., Addison Wesley Publishing Company, Inc., Reading, MA 1965, p. 127.

[24]Stone, G. M., "Trisonic Wind Tunnel Test of a .03 Scale Model of the Supersonic Transport to Investigate the Presure Distribution of Two Wing Configurations," North American Aviation, Inc., Los Angeles, CA, NA-63-1427, Dec. 1963.